Title

The excited state dynamics of protein-encapsulated Au nanoclusters

Authors

Shi, Jianying
Cooper, Jason K
Lindley, Sarah
et al.

Publication Date

2014-08-01

DOI

10.1016/j.cplett.2014.07.009

Peer reviewed

Chemical Physics Letters 610–611 (2014) 125–130

Contents lists available at ScienceDirect

Chemical Physics Letters

journal homepage: www.elsevier.com/locate/cplett

The excited state dynamics of protein-encapsulated Au nanoclusters

Jianying Shi[a,b,*], Jason K. Cooper[b], Sarah Lindley[b], Owen Williams[b], David S. Kliger[b], Yaolin Xu[c], Yuping Bao[c,*], Jin Zhong Zhang[b,*]

[a] Key Laboratory of Environment and Energy Chemistry of Guangdong Higher Education Institutes, School of Chemistry and Chemical Engineering, Sun Yat-sen University, Guangzhou 510275, China
[b] Department of Chemistry and Biochemistry, University of California, Santa Cruz, CA 95064, USA
[c] Department of Chemical and Biological Engineering, University of Alabama, Tuscaloosa, AL 35487, USA

ARTICLE INFO

Article history:
Received 30 May 2014
In final form 5 July 2014
Available online 11 July 2014

ABSTRACT

A combination of static and time-resolved spectroscopic techniques has been applied to study the low-lying excited electronic states of protein-encapsulated Au nanoclusters in terms of their energy levels and relaxation mechanisms. The energy levels were determined using photoluminescence (PL) spectroscopy. The excited state dynamics were probed using time-resolved PL techniques as well as femtosecond transient absorption (TA) spectroscopy. A simple model was proposed to account for the key spectral and dynamic features observed. This study has added new insight to the optical and dynamic properties of metal nanoclusters of interest in many applications including solar energy conversion and biomedical imaging.

1. Introduction

Gold (Au) nanoclusters containing a few tens of atoms have received a great deal of attention in the past decade for their potential application in biological imaging and labeling [1], optics [2], catalysis [3] and sensing [4]. Due to quantum confinement, the Au nanoclusters exhibit molecule-like discrete electronic states and unique optical and electronic properties that distinguish them from Au nanoparticles. A fundamental understanding of the electronic structure and excited state dynamics of Au nanoclusters is necessary to significantly improve their performance in technological applications.

There have been a number of investigations focused on the optical properties of Au nanoclusters, which are influenced greatly by the number of Au atoms in the cluster, the choice of ligand [5], and the oxidation state of Au [6]. Although Au nanoclusters have been extensively studied, the nature of their electronic structure remains unclear and its study is complicated by the dramatic difference between their excitation and absorption spectra. In fact, the specific electronic transitions responsible for the fluorescence observed are still under debate.

Protein-encapsulated Au nanoclusters have shown many advantages over other Au nanocluster systems, including green synthesis, biocompatibility, high water solubility, and the ease of further conjugation [7]. However, little work has focused on the influence of the protein templates on their optical properties. Furthermore, the mechanism of electronic relaxation of protein-encapsulated Au nanoclusters is not well understood.

In this work, the electronic structure and excited state dynamics of Au nanoclusters encapsulated in three model proteins, bovine serum albumin (BSA), lysozyme (LYS), and trypsin (TRY), are systematically investigated through static and time-resolved spectroscopy. The discrete energy levels are clarified for Au nanoclusters and the specific electronic transitions responsible for the blue and red emissions are identified. Finally, a model highlighting the major dynamic pathways for electronic relaxation is proposed based on the dynamics results obtained and analyzed.

2. Results

Absorption and PL spectra were used to probe the electronic structure of the Au nanoclusters. Figure 1 shows the static electronic absorption spectra of pure proteins and Au-proteins (Au nanoclusters encapsulated in proteins). A distinct absorption transition at 278 nm along with a featureless and broad absorption was observed for all Au-protein samples. For the protein only samples, only a 278 nm absorption band was observed. Figure 2 shows the photoluminescence (PL) (solid line) and PL excitation (PLE) (dashed

* Corresponding authors.
E-mail addresses: shijying@mail.sysu.edu.cn (J. Shi), ybao@eng.ua.edu (Y. Bao), zhang@ucsc.edu (J.Z. Zhang).

http://dx.doi.org/10.1016/j.cplett.2014.07.009
0009-2614/

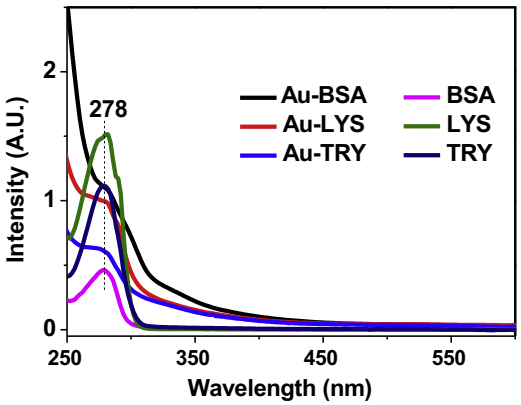

Figure 1. Absorption spectra of BSA, TRY and LYS proteins and Au nanoclusters encapsulated in proteins.

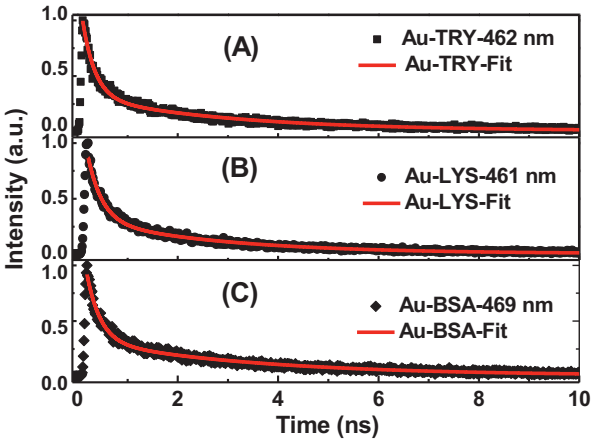

Figure 3. The blue emission decay profiles on the nanosecond time scale of Au-TRY (A); Au-LYS (B); and Au-BSA(C). The double exponential fitting curves of Au-proteins were added. Excitation wavelength: 390 nm.

line) spectra of the Au-proteins. Two different wavelengths, 500 nm and 388 nm, were used to excite the samples and produce the PL spectra. In Figure 2(A) with 500 nm excitation, a red band around 660 nm was observed in the PL spectra for all three samples, with different PL intensities. For 388 nm excitation in Figure 2(B), a blue band around 460 nm was observed in addition to the red one. The intensity ratio between the blue and red PL bands varied with the protein used. To explore the origin of these two emission bands, PLE spectra were monitored at the blue and red emission maximum and are shown as dashed lines in Figure 2. For the red emission, a 500 nm excitation band was observed in addition to three discernable bands at 280 nm, 325 nm, and 380 nm in Figure 2(A). For the blue band at about 460 nm, three excitation features at about 280 nm, 325 nm, and 380 nm were observed, as shown in Figure 2(B).

Although the steady-state spectra afford information about the electronic structure of Au nanoclusters, ultrafast time-resolved studies can provide further and complementary insight into the excited state dynamics. As such, time-resolved PL (TRPL) was utilized to probe the electronic relaxation in the excited electronic states in the Au nanoclusters. Figure 3 shows ns TRPL decay profiles of the blue emission at ~460 nm for the Au nanoclusters. All the decays are complete within about 10 ns. The decay curves are fit by a double exponential function as given by

$$y = A_1 \exp\left(\frac{-t}{\tau_1}\right) + A_2 \exp\left(\frac{-t}{\tau_2}\right) \quad (1)$$

where τ_1 and τ_2 represent the decay time constants, and A_1 and A_2 represent the respective amplitudes. The fitting results are shown in Table S1 in Supporting information. Two components of ~270 ps with 66% contribution and ~3 ns with 34% contribution were extracted from the decay traces of all three samples.

Figure 4(A) and (B) shows the TRPL decay traces of the red emission around 670 nm for the Au nanoclusters on the μs time scale pumped with 355 nm and 477 nm, respectively. All the decays are complete within 10 μs and the fitting results by a single exponential function are summarized in Tables S2 in Supporting information. About 1 μs lifetime was extracted for all three Au-proteins samples for both excitation wavelengths.

In addition, fs transient absorption (TA) has been used to gain insight into the early times dynamics. Figure 5 shows TA spectra of Au-LYS nanoclusters at different delay time (A/C) pumped with 390 nm and 490 nm excitation. Two-dimensional (2D) plots in terms of delay time and frequency are also included (B/D). In Figure 5(C) and (D), data points in the 450–500 nm range have been excluded as residual scattering from the pump beam could not be adequately deconvolved from the data. Following excitation, broad transient absorption (excited state absorption) features spanning the entire visible region (450–700 nm for 390 nm pump in Figure 5(A) and (B) and 500–700 nm for 490 nm pump in Figure 5(C) and (D) were observed. Au-TRY and Au-BSA samples exhibit similar broad TA features spanning the entire visible region (Figure S2), when pumped with either 390 nm or 490 nm.

To make it easier to visualize and analyze the TA data, Figure 6 shows the single-wavelength decay traces of Au nanoclusters pumped with 390 nm (A) and 490 nm (B). The kinetic data at 500, 550, 600 and 650 nm of Au-LYS exhibit an initial quick decay, followed by a medium relaxation and a final, slow decay extending

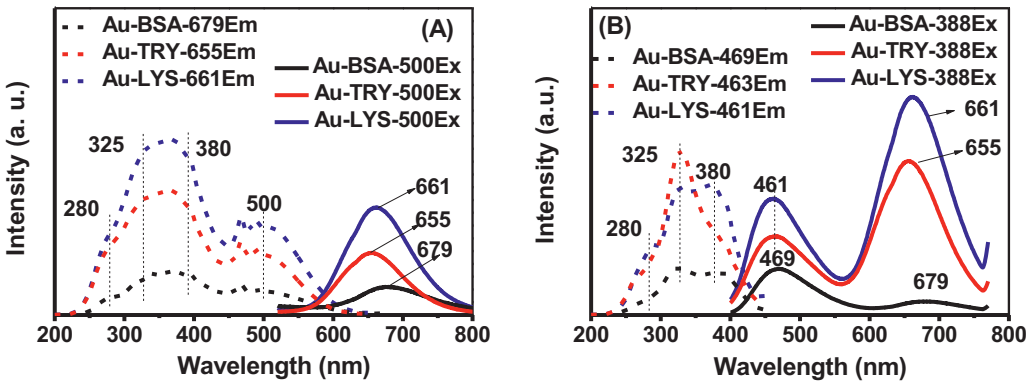

Figure 2. PL (solid line) and PLE (dash line) spectra of Au nanoclusters encapsulated in proteins. The excitation wavelength in PL is 500 nm (A) and 388 nm (B), and the PLE is monitored at the peak of the blue and red bands.

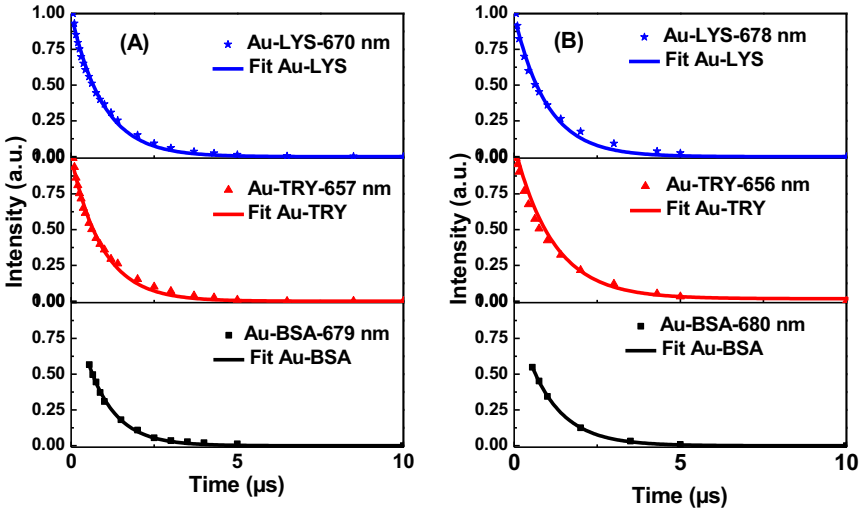

Figure 4. The red emission decay traces on the microsecond time scale with single exponential fitting curves for protein-encapsulated Au nanoclusters. Excitation wavelength: (A) 355 nm and (B) 477 nm.

out to 1450 ps. The decay profile of Au-LYS follows this trend when excited at 390 or 490 nm. When fit with a triple exponential decay function, three distinct decay components, ~1 ps, ~15 ps and >1450 ps, can be extracted, as shown in Table S4.

3. Discussion

In the static electronic absorption spectra, all three samples exhibit a distinct 278 nm (4.46 eV) absorption band along with a featureless and broad absorption. The 278 nm band can be attributed to the protein molecules in relation to the aromatic amino acid of tyrosine, tryptophan and phenylalanine [8]. The featureless and broad absorption is absent for the proteins alone and thus related to the Au clusters. In a previous study, the featureless and stepwise decreasing absorption was observed for BSA-Au nanoclusters with 25 Au atoms [9,10]. It was reported that molecular-like absorption of Au nanoclusters is highly sensitive to the nanocluster size and can serve as distinct spectroscopic

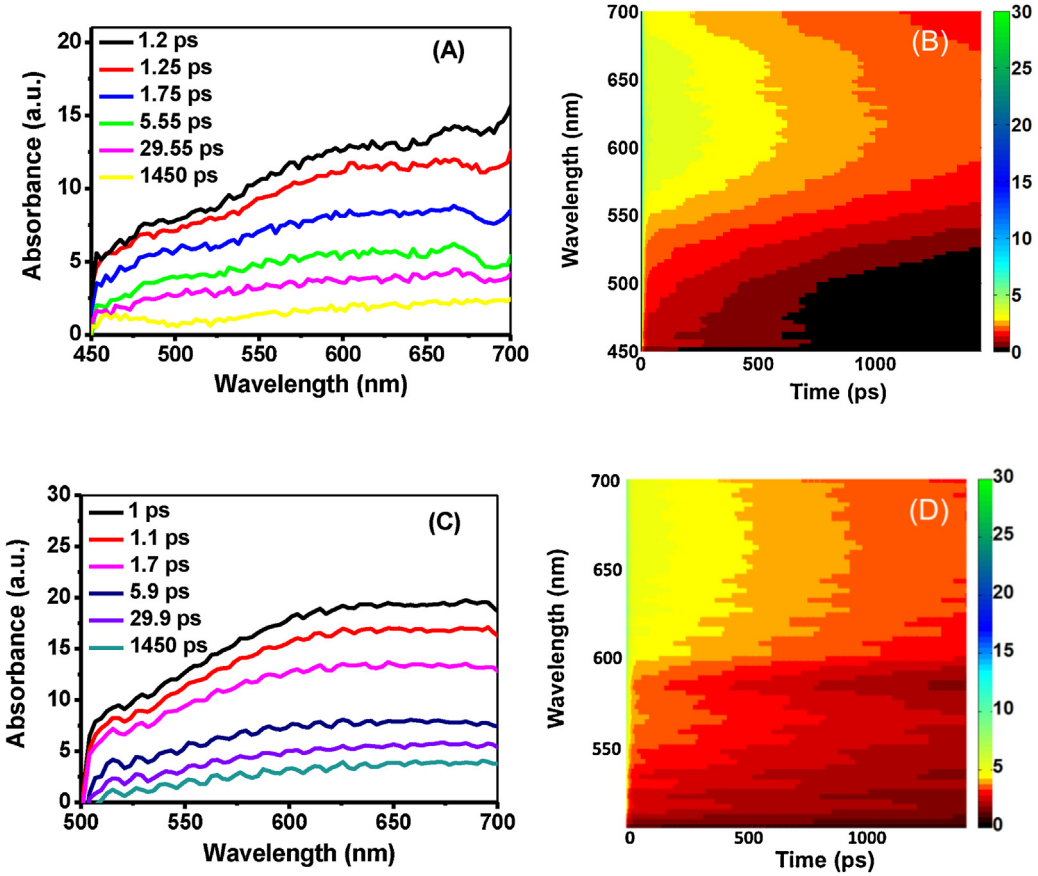

Figure 5. Transient absorption (TA) spectra of Au-LYS nanoclusters pumped over the 0–1450 ps delay ranges by 390 nm (A/B) and (490 nm (C/D). 2-D plots are of wavelength (nm) and delay (ps), with TA (mOD) represented by the color legend on the right of each figure. (For interpretation of the references to color in this figure legend, the reader is referred to the web version of the article.)

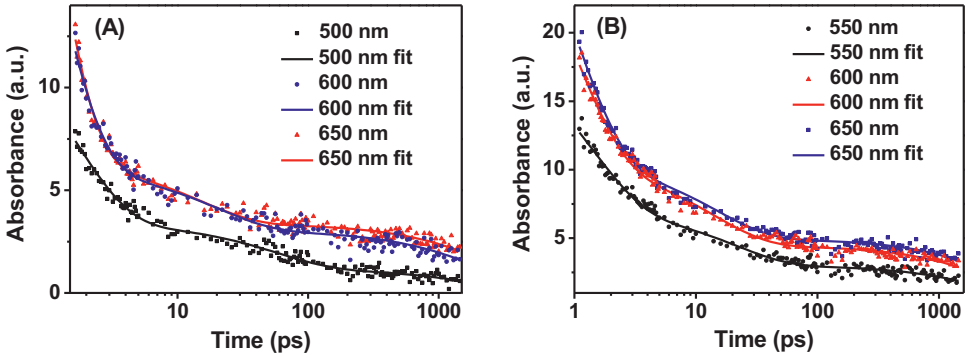

Figure 6. Kinetic data from transient absorption for Au-LYS at 500, 550, 600, and 650 nm, pumped by (A) 390 nm and (B) 490 nm.

fingerprints to identify the formation of Au nanoclusters with specific sizes [11]. Therefore, we propose that the core size of Au-protein samples responsible for the observed optical and dynamic properties in this study is 25 Au atoms. Mass spectra were not successfully obtained for our studies, because of the presence of extensive inorganic ions introduced during synthesis. However, a detailed study [12] on the size evolution of Au nanoclusters using a similar synthetic procedure has shown that the cluster size of Au-protein samples should be 25.

In addition to the absorption spectra, the PLE studies of Au nanoclusters can provide rich information about the electronic states and transitions involved. We focus on the 325, 380 and 500 nm PLE peaks that arise from the Au nanoclusters. In a previous study, an excitation band at about 353 nm was detected when 445 nm PL was monitored for Au nanoclusters capped with multivalent coordinating polymers (Au-MCP) [13]. In our case of Au-proteins, the 325 and 380 nm excitation bands are observed for the blue 460 nm emission. The different ligands in Au-MCP and Au-proteins may be responsible for the difference in peak positions. For the red emission, there are three PLE bands at 325, 380 and 500 nm for the Au nanoclusters, which are slightly different from the results of previous studies on BSA-Au nanoclusters that reported excitation peak at 480 nm [10], and two excitation peaks at 400 nm and around 500 nm [14], respectively. The small difference in PLE spectra (around 20 nm) may be due to different instruments or measurement conditions used, *e.g.* spectral distortion caused by different optical filters used.

Based on the PLE results, we assign the 500 and 380 nm excitation bands to transitions from the ground electronic state to the first and second singlet excited electronic states, respectively. This assignment is consistent with a previous report on BSA-Au nanoclusters, in which two excitation bands at 500 and 400 nm were attributed to transitions from the ground state to the first and a higher excited state, respectively [14]. The 325 nm excitation band could be a vibronic feature of the second excited electronic state. However, given the high density of electronic states in Au nanoclusters, it is more likely that the 325 nm band is due to transition from the ground state to the third excited electronic state of the Au nanoclusters.

PL is one of the most significant properties for Au nanoclusters considering its potential application. In previous PL studies, a red or near-infrared (NIR) emission, centered from 610 to 920 nm, was observed for Au_{38} [15], Au-BSA [14], Au_{55} [16], Au(I)–thiolate complex [17], and $Au_{25}(SG)_{18}$ nanoclusters [5,18]. This red band was suggested to be associated with the ligand [16,19]. Compared to the red/NIR emission, there have been relatively few reports concerning the blue emission of Au nanoclusters. The blue emission in Au-tripeptides and BSA-Au nanoclusters was ascribed to the aromatic side groups of the amino acid residues (tryptophan, tyrosine and phenylalanine) [10,14]. Nie et al. suggested that the 445 nm emission for Au nanoclusters capped with multivalent coordinating polymers was the ligand-to-metal electronic transition and not directly related to the intrinsic fluorescence properties of Au nanoclusters [13].

In our case, both a blue band at about 460 nm and a red band around 660 nm are observed for Au-proteins excited at 388 nm. The first absorption band of pure proteins is located at 280 nm with an onset at 305 nm, as shown in Figure 1, and the 388 nm excitation wavelength thus could not excite the proteins directly. Actually, a strong blue emission around 350 nm was observed for all three pure proteins in their PL spectra when excited at 280 nm (Figure S1), and the corresponding excitation band is located at 280 nm in the PLE spectra (Figure S1). This result is consistent with a previous study, in which the aromatic amino acids of tyrosine, tryptophan and phenylalanine in these three proteins were suggested as responsible for the PL and PLE processes [8]. Therefore, it is concluded that the pure proteins have a lowest PL band near 350 nm, and the blue emission of 460 nm originates primarily from the Au nanoclusters and is not strongly associated with the proteins.

It was reported that the PL of Au nanoclusters is influenced by the ligands coordinated with the Au core [5]. For Au nanoclusters encapsulated in three different proteins, the same cysteine residues in these proteins are used as ligands to stabilize Au nanoclusters [7]. As a result, no obvious ligand-dependence was observed for the emissions of Au-proteins. Except for BSA with 35 cysteine residues, the other two proteins have similar cysteine content (seven for TRY and eight for LYS). This could be the reason for the similar blue bands observed for Au-TRY (463 nm, 2.68 eV) and Au-LYS (461 nm, 2.69 eV), and also account for the 0.03 eV difference between Au-BSA (469 nm, 2.65 eV) and Au-TRY (463 nm, 2.68 eV). As opposed to the blue band, a larger shift was observed for the red band, *e.g.* 0.07 eV shift between Au-TRY (655 nm, 1.90 eV) and Au-BSA (679 nm, 1.83 eV), and 0.02 eV shift between Au-TRY (655 nm, 1.90 eV) and Au-LYS (661 nm, 1.88 eV). This result indicates that the red emission is more sensitive to the details of the ligands involved.

The PL lifetime is directly related to the electronic transition nature of Au nanoclusters. For the two decay components of ~270 ps and ~3 ns observed for the blue emission, the ~3 ns component is similar to the 2.5 ns lifetime observed by Tang et al. in the dynamic study of BSA-Au for the blue band centered at 470 nm [20]. The ~1 μs lifetime for the red emission, independent of the excitation wavelength at 355 nm or 477 nm, indicate that the emission originates from the same electronic state even though the initial state is different immediately following photoexcitation. The two separate PL bands with different lifetimes were also reported in the studies of monolayer-protected Au clusters (MPCs)[16] and $Au_{28}(SG)_{16}$ [21]. The short-lived visible emission in Au MPCs was ascribed to the transition from a.higher lying excited state to the ground state and the long-lived NIR emission was attributed to surface-related states [16]. The two luminescence bands for $Au_{28}(SG)_{16}$ with maxima around 1.5 eV (828 nm) and

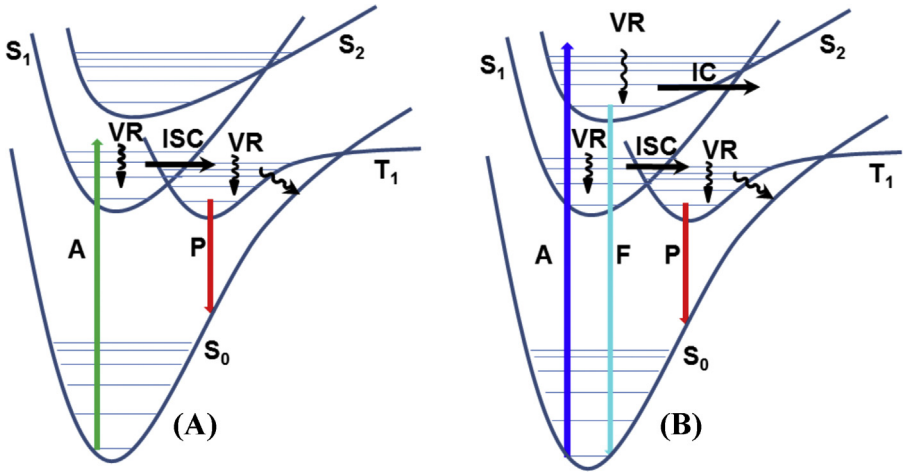

Figure 7. Schematic energy level diagram and proposed major electronic relaxation pathways in Au nanoclusters. The left panel (A) is for visible excitation, *e.g.* 500 nm that first populates the first excited singlet electronic state, while the right panel (B) is for near UV excitation, *e.g.* 380 nm that first populates the second excited singlet electronic state. A – absorption, F – fluorescence, P – phosphorescence, IC – internal conversion, ISC – intersystem crossing, VR – vibrational relaxation, S – singlet state, T – triplet state.

1.15 eV (1080 nm) were assigned to fluorescence and phosphorescence, related to a singlet and triplet excited state of the molecular-type cluster, respectively [21]. We suggest that the short-lived blue emission originates from the second excited singlet state (S_2) of Au nanoclusters while the long-lived red emission starts primarily from the excited triplet state, as discussed in more detail later.

It has been indicated above that the first excited singlet state (S_1) of the Au-proteins is located near 500 nm. As PL is usually red-shifted in peak position compared to absorption, the 460 nm blue emission with energy higher than 500 nm must thus originate from S_2. In previous studies, it was reported that the singlet and triplet states have a small energy gap of 30.6 ± 1.9 meV in BSA-Au [14]. A different study concluded that the singlet and triplet states in glutathione-protected Au nanoclusters were degenerate energy levels [22]. These reports seem to suggest that an efficient intersystem crossing occurs and the excited electron quickly crosses into the first triplet state (T_1) from S_1. Our TA results also indicate fast intersystem crossing, which would account for the lack of emission from S_1.

The TA spectra provide more detailed information about the excited state dynamics of Au-proteins. In a previous study of BSA-Au, Tang et al. reported a broad transient absorption with 2 ps, hundreds of ps and a μs lifetime [14]. In our case, the TA profiles feature a fast (~1 ps), an intermediate (tens of ps), and a slow (>1 ns) decay (limited by the translation stage used). The fast decay in Tang's work was ascribed to surface/defect state trapping [14]. In the study of rod-shaped Au_{25} nanoclusters, a 0.8 ps component was attributed to fast internal conversion from LUMO + *n* to LUMO [23]. In our case, the 1 ps decay is tentatively attributed to vibrational relaxation within excited singlet states or internal conversion from S_2 to S_1. The long-lived component does not significantly decay in the measurement window (1.5 ns), which could correspond to the μs component assigned to the triplet state decay back to the ground state, similar to what has been reported in the studies of BSA-Au [14] and Au_{25} nanoclusters [23]. For the intermediate component with tens of ps lifetime, we assign it to the intersystem crossing between relaxed S_1 and T_1, which is shorter than the time scale of hundreds of ps reported for BSA-Au [14], possibly due to difference in the protein, LYS *vs* BSA.

At present, several models have been proposed to explain the origin of the two PL band of Au nanoclusters, including the solid state model and molecular model [16,19,22]. Based on the previous models and our results, a model for the electronic structure of Au nanoclusters is proposed and shown in Figure 7. Also illustrated are the major pathways for electronic relaxation proposed in accordance with all the dynamics data. Following 490 nm excitation as shown in Figure 7(A), the electron is promoted into S_1, and nonradiative vibrational relaxation in S_1 state occurs within about 1 ps. Then, intersystem crossing from S_1 to T_1 occurs on the time scale of about 15 ps. Finally, decay from T_1 to S_0 occurs with a 1 μs lifetime, resulting in the red PL.

When excited at 390 nm, as shown in Figure 7(B), the electron is directly excited to S_2, which vibrationally relaxes on the time scale of about 1 ps. At the same time, internal conversion from S_2 to S_1 occurs. Subsequently, the electron in S_1 can vibrationally relax and, at the same time, intersystem cross to T_1 on the time scale of about 15 ps, similar to the situation with 490 nm excitation. Finally, the electron decays from T_1 to S_0, with a lifetime of about 1 μs. In the meantime, the electron in the vibrational ground state of S_2 can directly decay to S_0, generating the blue emission. The 270 ps and 3 ns time constants observed in TRPL are primarily due to the complex relaxation kinetics of S_2 that is tied with S_1, T_1 and S_0. The complexity of the kinetics is partly due to the reversible nature of the internal conversion and intersystem crossing processes. It should be mentioned that the fast nonradiative decay due to vibrational relaxation and internal conversion dominates the excited state relaxation (~80% by amplitude based on fitting of the TA dynamics data), which is consistent with the relatively weak blue emission observed. The fact that the long-lived excited states in Au nanoclusters can be generated by both UV and visible light excitation makes Au nanoclusters potentially useful as light harvesters, photosensitizers, and electron donors in photocatalysis [24].

4. Conclusion

In conclusion, the molecular-like energy levels involved in singlet and triplet excited states of the protein-encapsulated Au nanoclusters are elucidated according to their static spectra and time-resolved measurements. To account for all the key spectral and dynamic features, a simple model is proposed for the relevant electronic states involved. When excited into the S_1 directly, vibrational relaxation occurs first, followed by intersystem crossing to the triplet state (T_1), and finally decay to the ground state (S_0), *via* radiative, leading to the red emission, and non-radiative processes. When excited into the S_2 state, fast vibrational relaxation is followed by fast international conversion from S_2 to S_1 during and after vibrational relaxation in S_2. Once in S_1, the dynamics are similar to that observed for direct excitation into S_1 by light.

In competition with S_2 to S_1 internal conversion following vibrational relaxation in S_2, the electron in S_2 can directly relax to S_0 radiatively, leading to the blue emission, or non-radiatively *via* S_2 to S_0 internal conversion through S_1 and T_1. The major relaxation pathways of the excited states do not seem to be strongly affected by the different proteins, indicating that they are dominated by the electronic properties of the Au nanoclusters. This work provides important new insight into the excited state dynamics of Au nanoclusters.

Supporting information

Synthesis and experimental details are furnished. PL and PLE spectra of proteins, kinetic data from time-resolved fluorescence and transient absorption, and transient differential absorption spectra of Au-TRY and Au-BSA are included.

Acknowledgments

The research was financially supported by the US NSF-ECCS 0823921, NSF-DMR 0907204 and DMR1149931. The 973 Program (2014CB845600), the NSF of China (No. 21103235), NSF of Guangdong Province (No. S2012010010775), and Science and Technology Program of Guangzhou City (No. 2013J4100110). S.A. Lindley acknowledges support from the W.M. Keck Center for Nanoscale Opto-fluidics at UC Santa Cruz.

Appendix A. Supplementary data

Supplementary material related to this article can be found, in the online version, at doi:10.1016/j.cplett.2014.07.009.

References

[1] N.L. Rosi, D.A. Giljohann, C.S. Thaxton, A.K.R. Lytton-Jean, M.S. Han, C.A. Mirkin, Science 312 (2006) 1027.
[2] H. Fan, et al., Science 304 (2004) 567.
[3] N. Zheng, G.D. Stucky, J. Am. Chem. Soc. 128 (2006) 14278.
[4] H. Wohltjen, A.W. Snow, Anal. Chem. 70 (1998) 2856.
[5] Z. Wu, R. Jin, Nano Lett. 10 (2010) 2568.
[6] H.F. Qian, M.Y. Sfeir, R. Jin, J. Phys. Chem. C 114 (2010) 19935.
[7] Y.L. Xu, J. Sherwood, Y. Qin, D. Crowley, M. Bonizzoni, Y.P. Bao, Nanoscale 6 (2014) 1515.
[8] F.W.J. Teale, Biochem. J. 76 (1960) 381.
[9] Y. Yu, Z.T. Luo, C.S. Teo, Y.N. Tan, J.P. Xie, Chem. Commun. 49 (2013) 9740.
[10] J.P. Xie, Y.G. Zheng, J.Y. Ying, J. Am. Chem. Soc. 131 (2009) 888.
[11] C.Y. Tay, Y. Yu, M.I. Setyawati, J.P. Xie, D.T. Leong, Nano Res. (2014), http://dx.doi.org/10.1007/s12274-014-0441-z.
[12] K. Chaudhari, P.L. Xavier, T. Pradeep, ACS Nano 5 (2011) 8816.
[13] H.W. Duan, S. Nie, J. Am. Chem. Soc. 129 (2007) 2412.
[14] X.M. Wen, P. Yu, Y.R. Toh, A.C. Hsu, Y.C. Lee, J. Tang, J. Phys. Chem. C 116 (2012) 19032.
[15] J.T. Wijngaarden, O. Toikkanen, P. Liljeroth, B.M. Quinn, A. Meijerink, J. Phys. Chem. C 114 (2010) 16025.
[16] S.H. Yau, O. Varnavski, J.D. Gilbertson, B. Chandler, G. Ramakrishna, T. Goodson III, J. Phys. Chem. C 114 (2010) 15979.
[17] Z.T. Luo, X. Yuan, Y. Yu, Q.B. Zhang, D.T. Leong, J.Y. Lee, J.P. Xie, J. Am. Chem. Soc. 134 (2012) 16662.
[18] E.S. Shibu, M.A.H. Muhammed, T. Tsukuda, T. Pradeep, J. Phys. Chem. C 112 (2008) 12168.
[19] M.S. Devadas, J. Kim, E. Sinn, D. Lee, T. Goodson III, G. Ramakrishna, J. Phys. Chem. C 114 (2010) 22417.
[20] X.M. Wen, P. Yu, Y.R. Toh, J. Tang, J. Phys. Chem. C 116 (2012) 11830.
[21] S. Link, A. Beeby, S. FitzGerald, M.A. El-Sayed, T.G. Schaaff, R.L. Whetten, J. Phys. Chem. B 106 (2002) 3410.
[22] C. Zhou, C. Sun, M.X. Yu, Y.P. Qin, J.G. Wang, M. Kim, J. Zheng, J. Phys. Chem. C 114 (2010) 7727.
[23] M.Y. Sfeir, H. Qian, K. Nobusada, R. Jin, J. Phys. Chem. C 115 (2011) 6200.
[24] K.G. Stamplecoskie, Y.S. Chen, P.V. Kamat, J. Phys. Chem. C 118 (2014) 1370.